

Secular, Transient, and Seasonal Crustal Movements in Japan from a Dense GPS Array

IMPLICATION FOR PLATE DYNAMICS IN CONVERGENT BOUNDARIES

■ Kosuke Heki

Abstract

The Japanese nationwide dense array of Global Positioning System (GPS) receivers has been yielding large amounts of crustal movement data in Japan over the last decade. In this paper, I review its contribution to our knowledge of crustal dynamics in a subduction zone. The secular velocity field provides information on rigid plate motion and coupling on the plate interface and allows us to discuss seismic moment budgets and recurrence intervals of large interplate earthquakes. The Japanese Islands are divided into two plates colliding with each other in the central Japan, and this causes complex seismicity along the Nankai-Suruga Trough, especially in the Tokai area. Three-dimensional velocity profiles across northeastern Japan show unexpected secular subsidence of the fore-arc region. This might be a manifestation of deep basal subduction erosion of the upper plate by the subducting slab. The GPS array has revealed many coseismic and postseismic fault slips, some of which were slow and aseismic. In northeastern Japan, most interplate earthquakes are followed by after slip over the regions surrounding the ruptured asperities. Acceleration and deceleration of creeping movement of plate interface can also be inferred from activities of small repeating earthquakes, which represent ruptures of small isolated asperities within the region of stable or conditionally stable frictional properties. In southwestern Japan, slow slip tends to occur as independent silent earthquakes. Some of them are quasi-periodic and are often accompanied by nonvolcanic deep tremors. Seasonal crustal movements are caused by changes of various kinds of surface loads, among which snow loading is by far the largest. Understanding seasonal movements is important in order to isolate subtle signals of transient phenomena from the raw data, and to investigate the possible causal relationship between surface loads and seasonal changes in seismic activities.

Introduction

Space geodetic techniques such as very long baseline interferometry (VLBI), satellite laser ranging (SLR), Global Positioning System (GPS), and interferometric synthetic aperture radar (InSAR) have been the main tool to study crustal movements for nearly 20 years. The benefits of GPS among such techniques are (1) the relatively inexpensive ground stations (receiver and antenna), (2) a modest amount of raw data, and (3) a dense sampling in time. Point 1 makes GPS suitable for dense deployment of receiving stations in tectonically active regions, while point 2 enables the exchange of data through Internet or public telephone line for rapid data analysis in a central station. InSAR provides data much denser in space, but owing to the need for almost identical orbits over studied areas, its temporal sampling is sparse. In contrast, point 3 enables GPS receivers to be used as long period seismometers, recording displacements associated with passage of seismic waves [Larson *et al.*, 2003]. In this respect, GPS and InSAR are complementary; *i.e.*, the two techniques are especially powerful when combined.

The dense GPS array, GEONET (GPS Earth Observation Network), deployed over the Japanese Islands by Geographical Survey Institute (GSI) started operation in 1993. The number of sites has been increasing since then and attained ~1200 sites in 2004 (fig.16.1). The RINEX (Receiver Independent Exchange format) raw data, as well as official solutions obtained by the Bernese software with the analysis strategy described by *Hatanaka* [2003b], can be obtained freely from GSI's Web site (<http://www.gsi.go.jp>).

There is a standard framework to interpret crustal deformation in convergent plate margins. Secular crustal movement from tectonic plate motion is overprinted with interseismic crustal deformation due to elastic loading by the subducting slab. A substantial part of the interseismic displacement accumulated over an earthquake cycle is considered to be canceled instantaneously by coseismic movement of the next earthquake, *i.e.*, coseismic and interseismic movements are approximately opposite in direction and equal in magnitude. Recent geodetic observations have shown that this simple model is valid as a first approximation. However, there are examples that do not match this model. These include transient crustal deformation associated with slow fault slip, seasonal crustal deformation, subsidence not canceled over an earthquake cycle, and so on. In this paper I review crustal dynamics in Japan revealed by GEONET emphasizing such nonstandard phenomena and their geophysical implications.

Secular Crustal Movements

The Japanese Islands used to be thought to reside on the Eurasian Plate (EU), with two oceanic plates, namely the Pacific (PA) and the Philippine Sea (PH)

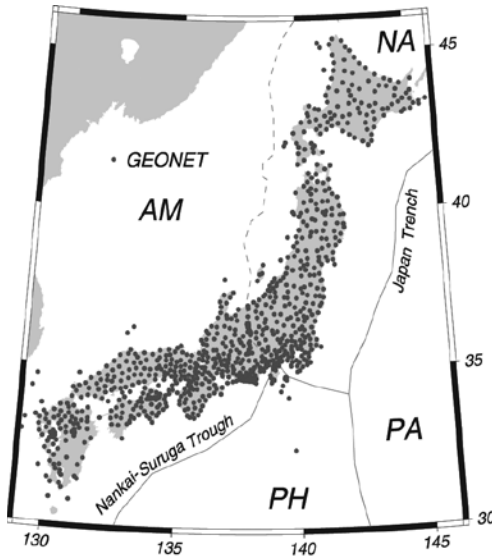


Figure 16.1 Distribution of the GEONET GPS stations and plate tectonic setting of the Japanese Islands. Abbreviations are the North American (NA), Pacific (PA), Amurian (AM), and the Philippine Sea (PH) plates.

plates, subducting at the Japan Trench and the Nankai Trough, respectively. A new plate boundary was proposed along the eastern margin of the Japan Sea and central Japan, which divides the country into two plates colliding with each other [Nakamura, 1983; Kobayashi, 1983] (fig. 16.1). This was originally considered to be the boundary between EU and the North American plate (NA). Later, *Seno et al.* [1996] suggested that northeastern Japan (NEJ) is a part of the newly proposed Okhotsk plate (OK). GPS observations in Korea, Russia, China, and southwestern Japan (SWJ) showed significant eastward components relative to the stable interior of EU. *Heki et al.* [1999] attributed this to the eastward movement of the Amurian plate (AM), covering SWJ, Korean Peninsula, northeastern China, Russian Far East, at a rate of 9–10 mm/yr with respect to EU. They also suggested that NEJ is a part of NA rather than OK and collides with SWJ at a rate of ~20 mm/yr in central Japan. Later, *Sagiya et al.* [2000] identified the concentration zone of compressional strain running from Niigata to Kobe from velocity fields obtained by GEONET and named it the Niigata-Kobe Tectonic Zone (fig. 16.2). AM has offered a good platform to model the interseismic velocity field in SWJ caused by the subduction of PH at the Nankai Trough [Miyazaki and Heki, 2001].

Recurrence of Interplate Earthquakes Along the Nankai/Suruga Trough

The fact that Japan consists of two plates colliding with each other has significant implications for seismotectonics in Japan, especially for interplate earthquakes along the Nankai-Suruga Trough. There, *M* 8 class interplate thrust events have occurred repeatedly during the last 1500 years with an average

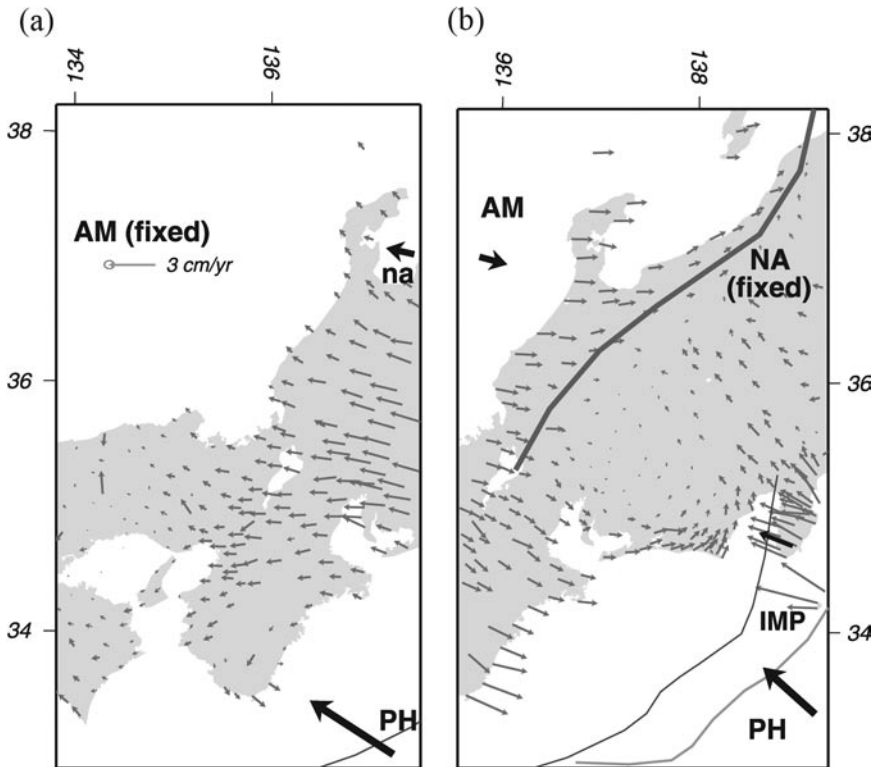


Figure 16.2 Long-term velocity fields of central Japan in the frames fixed to (a) AM and (b) NA. Thin gray arrows and thick black arrows show observed velocities at GPS sites and those predicted by Euler vectors. The northern most tip of PH is suggested to be detached from the rest as the Izu Microplate (IMP). Niigata-Kobe Tectonic Zone [Sagiya *et al.*, 2000] is shown by a gray broad line. The typical error ellipse size is indicated at the arrowhead of the legend vector.

recurrence interval of 120 years [Sangawa, 1993]. The next large event is anticipated in the Tokai district (the easternmost segment of the trough) since the last major events, the 1944/1946 Tonankai/Nankaido earthquakes, ruptured the rest of the trough [Ishibashi, 1981]. This seismic gap hypothesis, however, assumes that both the landward and oceanic sides of the trough are single plates. Transition between AM and NA somewhere in the landward plate implies along-trough differences in plate convergence rates. Sagiya [1999] pointed out that the incipient plate convergence along the Zenisu Ridge and detachment of the northern tip of PH as the Izu Microplate causes further complexities in convergence rates.

Heki and Miyazaki [2001] suggested that the convergence rate at the Tokai district is reduced to only $\sim 1/3$ of the rate at the western segments by two factors, (1) the landward plate belongs to NA rather than AM, and (2) the Izu

Microplate subducts there instead of PH. A smaller convergence rate makes the recurrence interval longer. This can be confirmed in past records (fig. 16.3, bottom), where the Tokai segment often fails to rupture just like it did in the last cycle. *Sagiya* [1999], by inversion of GPS data, inferred the slip deficit to be 30–40 mm/yr in the Sea of Enshu and 25–30 mm/yr in Suruga Bay, smaller than the PH-AM convergence rate, consistent with *Heki and Miyazaki* [2001] (fig.16.3, top).

Using a larger data set of GPS observations in Siberia, *Kogan et al.* [2000] suggested that a newly determined Euler pole of EU can account for velocity vectors in Europe and in eastern Asia simultaneously and dismissed the exis-

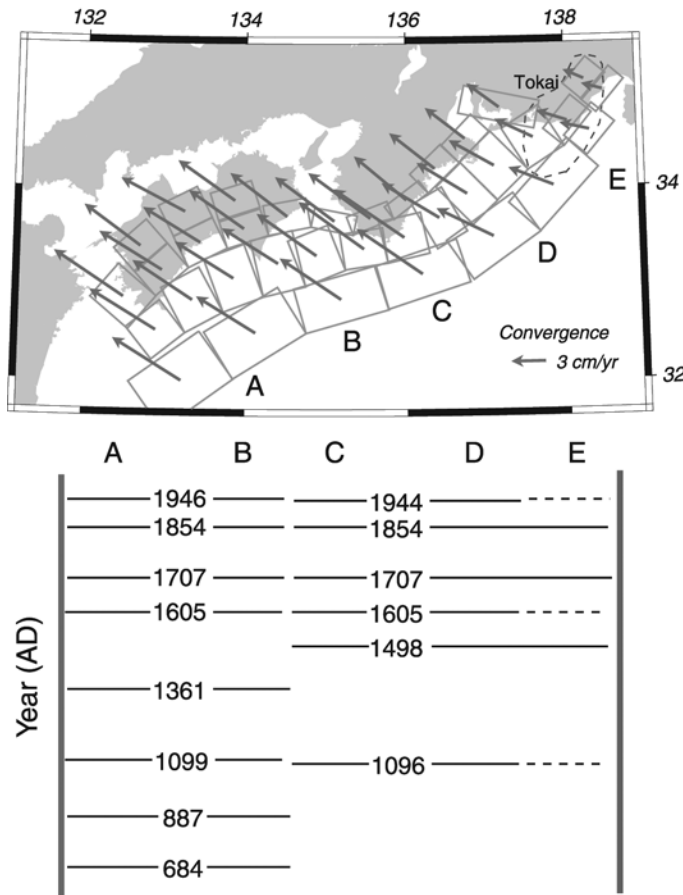


Figure 16.3 Plate convergence vectors at the centers of the fault segments along the Nankai-Suruga Trough. Convergence vectors are significantly shorter in the expected focal region of the future Tokai earthquake shown by the dashed line. The lower part shows years (AD) of occurrences of historic interplate thrust events for five segments along the trough, A, B, C, D, and E [*Sangawa*, 1993]. The Tokai region corresponds to segment E.

tence of AM. Additional velocity data between Europe and the Far East would help to solve this problem: should the Euler vector for EU be revised or is it similar to the NUVEL-1 result [DeMets *et al.*, 1990] implying several smaller plates in eastern Asia? Such an uncertainty in the large-scale plate tectonic setting has little effect on geodetic interpretation in the Japanese Islands, i.e., they are composed of two plates colliding with each other in central Japan, and convergence rates vary along the Nankai-Suruga Trough.

Interplate Coupling and Vertical Velocities

Interseismic crustal deformation due to a locked plate interfaces in subduction zones is often modeled as the sum of steady-state reverse slip and normal slip at the locked surface [Savage, 1983]. We often disregard crustal deformation by the former, and model interseismic deformation assuming only the latter hypothetical slip, referred to as back slip or slip deficit. The interseismic velocity field provides information on the distribution of slip deficits (i.e., strength of plate coupling) at seismogenic depths of the plate interface. Crustal strain observed by GPS suggests a rather simple view that the plate interface is almost fully coupled over the depths 5–50 km in NEJ and 5–25 km in SWJ. Coupling gradually decreases and disappears at the depths of 65 km in NEJ and 35 km in SWJ [Mazzotti *et al.*, 2000]. However, Nishimura *et al.* [2000] and Suwa *et al.* [2003] suggested nonuniform distribution of slip deficits in NEJ, i.e., stronger coupling in the regions where relatively large asperities exist [Yamanaka and Kikuchi, 2004].

The majority of past studies have been based only on horizontal crustal movements or strains because of the much lower signal-to-noise ratio of vertical signals. However, increasing observation periods are making it possible to discuss secular uplift or subsidence rates. Aoki and Scholz [2003] confirmed that the observed vertical crustal velocity field in SWJ is consistent with the back-slip model predictions, i.e., the area closest to the trough subsides, and the subsidence changes to uplift across the “hinge line.” Uplift decays as we go farther inland (see the velocity profile discussed in the next section). The largest uplift occurs approximately at the surface projection of the lower limit of the coupled zone. At the same time, Aoki and Scholz [2003] did not find such a pattern in NEJ; i.e., sites along the Pacific coast subsides secularly by a few millimeters per year, decaying toward the west. They did not discuss this issue in much detail and attributed the absence of the uplift zone to the remoteness of the shoreline from the trench (i.e., uplifted zone lies offshore).

Tide gauge data at Ayukawa (see fig. 16.6 for location) provide an example of the peculiar situation of NEJ (fig. 16.4). The data span >40 years and record the last interplate event, the 1978 Miyagi-Oki (*M* 7.3) earthquake. According to the basic concept of interseismic crustal deformation, cumulative displacement during the recurrence interval is to be canceled substantially by the next coseismic displacement. The Ayukawa tide gauge data violate this concept;

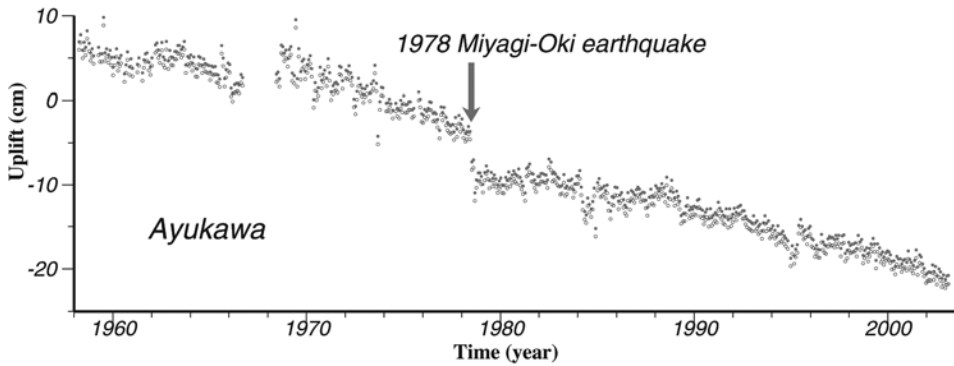


Figure 16.4 Ayukawa (fig. 16.6) tide gauge data converted to show the land uplift. Secular sea-level change due to eustatic sea-level rise of ~ 1.9 mm/yr (fig. 16.6) was removed from the time series. The data show coseismic subsidence in the 1978 event as well as interseismic slow subsidence. This example violates the classical concept that the coseismic jump cancels the cumulative interseismic displacement.

the site slowly subsides during the interseismic period and coseismic subsidence is added when an earthquake occurs. Figure 16.5 shows secular vertical velocities derived from the daily coordinates of GEONET 1996.2–2000.5 by modeling the time series with linear and seasonal (annual and semiannual) components. As shown by *Aoki and Scholtz* [2003], GPS points along the Pacific coast of NEJ show secular subsidence. In the next section, I will confirm the accuracy of vertical velocity results obtained by GPS by comparing them with sea-level rise data.

Secular Subsidence of the NEJ Fore Arc

Figure 16.6 compares long-term sea-level change rates at 76 tide gauges [*Geographical Survey Institute* 2002] obtained after removing oceanographic signals using *Kato's* [1983] method, and vertical velocities of nearby GPS points. Absolute vertical velocities (those relative to the Earth's center of gravity) of GPS points were obtained by fixing the Tsukuba velocity to the value given in the International Terrestrial Reference Frame (ITRF) 2000 [*Altamimi et al.*, 2002]. They are negatively correlated with an offset (sea-level rise is larger) of ~ 1.9 mm/yr, which agrees with the eustatic sea-level rise expected in this region [*Mitrovica et al.*, 2001]. The large scatter about the regression line may reflect (1) different time spans represented by the two techniques, (2) local differences of vertical velocities between tide gauges and GPS sites, and (3) underestimation of vertical rate errors from tide gauges.

We now compare horizontal (normal to trench strike) and vertical velocity profiles of NEJ (fig. 16.7) and SWJ (fig. 16.8) with the velocities predicted by the slip deficit model [*Savage*, 1983] assuming the depth-dependent cou-

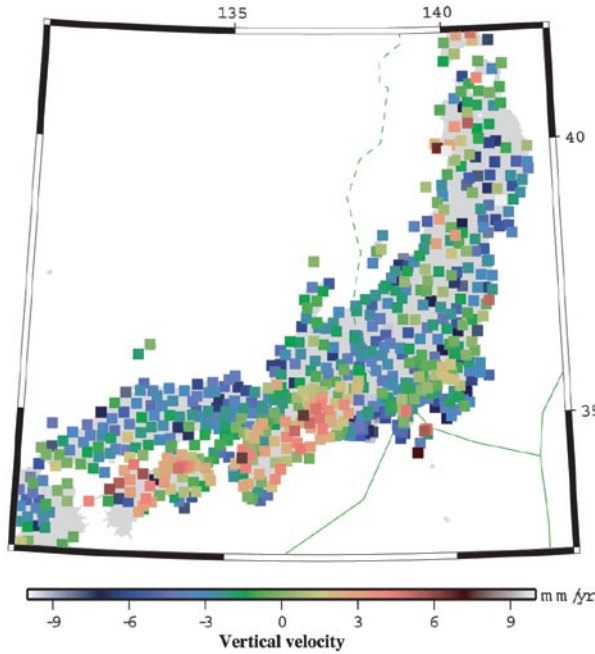


Figure 16.5 Vertical velocities of the GEONET GPS points. The vertical velocity of the reference station (Tsukuba) was fixed to the value given in ITRF2000 [Altamimi et al., 2002], and these velocities are hence relative to the geocenter.

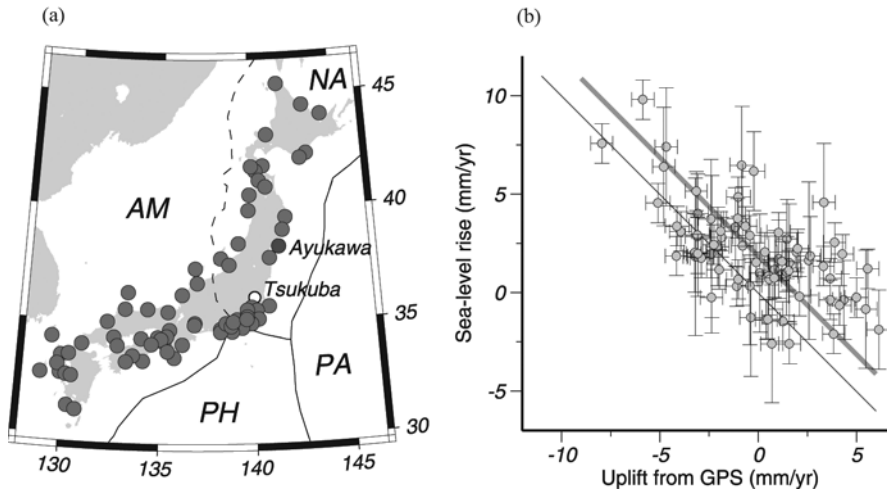


Figure 16.6 Comparison of vertical velocities from GPS and tide gauges. (a) Dots denote tide gauge stations. Sea-level rise at tide gauges and vertical velocities at nearest GPS sites are negatively correlated with a small excess sea-level rise of 1.9 mm/yr (offset between the best-fit thick gray line and the thin line) corresponding to the (b) eustatic sea-level rise in Japan. Errors for GPS velocities are 1σ (error of Tsukuba velocity in ITRF2000 [Altamimi et al., 2002] is considered), and those for tide gauges are ± 1 , ± 2 , ± 3 , and ± 4 mm/yr for sites observed for >40 , >30 , >20 , and <20 years, respectively.

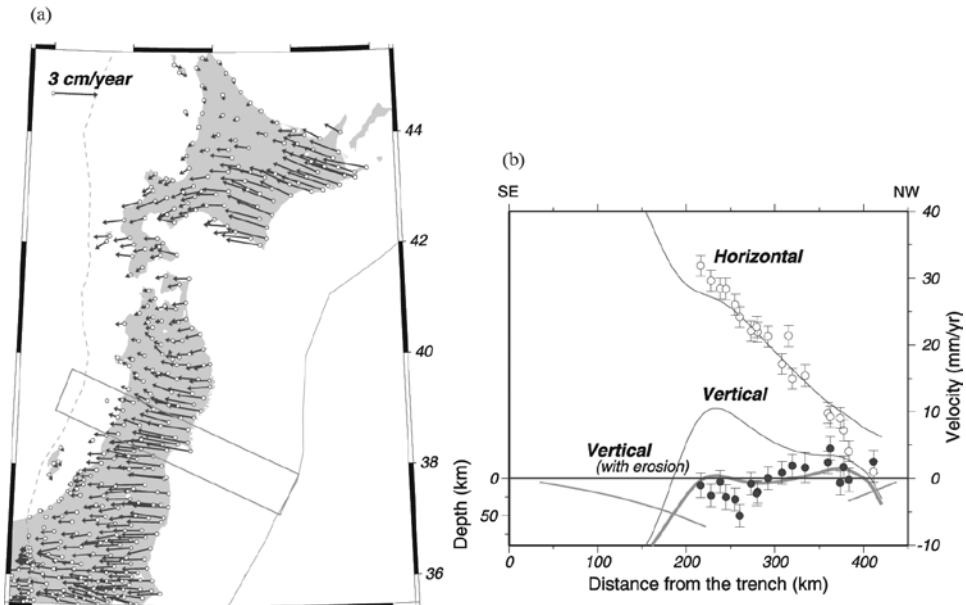


Figure 16.7 Comparison of observed and calculated velocities in NEJ. (a) Trench-normal horizontal (open circles), and vertical (solid circles) velocities in green rectangles plotted against (b) the distance from the Japan Trench. Curves are the velocity profiles predicted by the slip deficits at the plate interface, whose cross section is shown with gray curves. Error bars show 3σ . Another heavier gray curve, indicated as “with erosion,” is the vertical profile obtained taking account of tectonic erosion of 15 mm/yr over the depths 45–90 km.

pling strength after *Mazzotti et al.* [2000]. Euler vectors derived by space geodesy were used to calculate convergence vectors at NEJ [*Altamimi et al.*, 2002] and SWJ [*Miyazaki and Heki*, 2001], assuming NA-PA and AM-PH plate pairs, respectively. Along the eastern margin of the Japan Sea, we considered additional convergence between AM and NEJ, whose convergence vector was taken from *Heki et al.* [1999]. Slab geometry is assumed to be similar to fault planes of past earthquakes along this zone, e.g., the 1983 Central Sea of Japan earthquake [*Earthquake Research Committee*, 1998]. The vertical velocity reference is reasonably defined by the geocenter, but selecting horizontal references is not straightforward. For SWJ, I fixed Kamitsushima (fig. 16.8), which is >500 km distant from the Nankai Trough. In NEJ, because subduction occurs at both sides of Japan, a stable reference cannot be found within the arc. There an artificial translation is given to the horizontal velocity profile to let them match the prediction.

In SWJ, both horizontal and vertical crustal movements are consistent with the model predictions (fig. 16.8) as suggested by *Aoki and Scholtz* [2003]. In NEJ, however, vertical velocities show subsidence relative to the model (fig. 16.7).

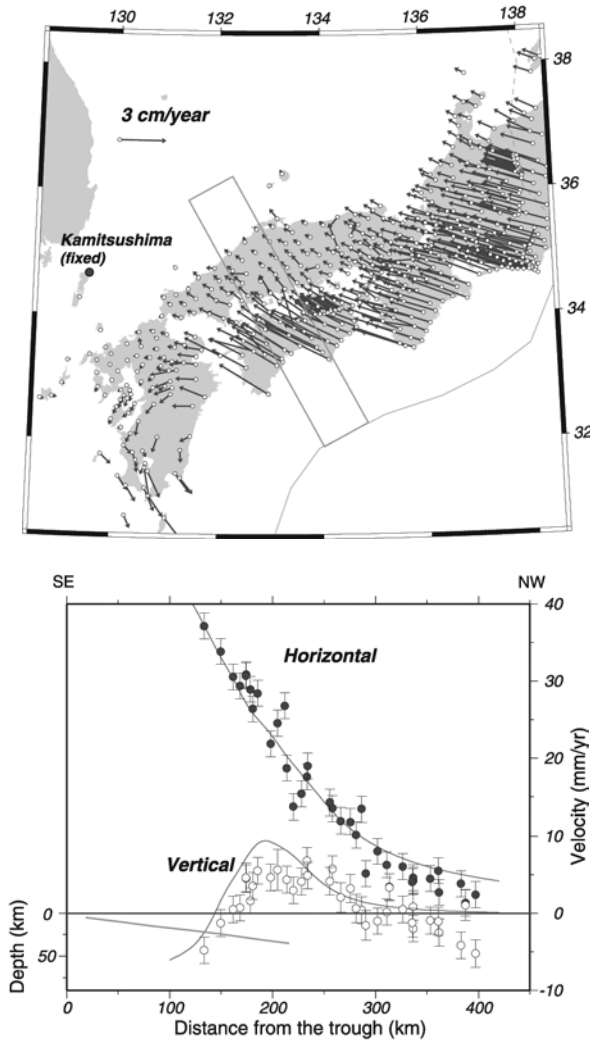


Figure 16.8 Comparison of observed and calculated velocities in SWJ. Unlike NEJ (fig. 16.7), both horizontal and vertical velocity profiles are consistent with the model curves.

This anomaly might indicate a viscous effect; i.e., crustal velocity may vary during an earthquake cycle due to viscous relaxation in an asthenosphere. Cohen [1994] calculated such cyclic components for several cases. He showed that viscous effects modulate interseismic displacement rates to some extent but rarely change directions; i.e., the uplift/subsidence pattern remains similar throughout the cycle. Tide gauge data in Ayukawa (fig. 16.4) provide additional insight. Although there is some difference between the rates immediately before and after the 1978 event, the site subsides persistently throughout

the cycle. It is hence unlikely for viscous effects to cause the fore-arc subsidence observed in NEJ. Another possibility is that we applied an incorrect coupling strength in the model. We could make the fore arc subside, by extending the coupled (i.e., seismogenic) zone to the depth of 100–120 km [Suwa *et al.*, 2003]. However, this is inconsistent with our knowledge that interplate thrust earthquakes occur at depths shallower than 50–60 km in NEJ [Hasegawa *et al.*, 1991] and most other regions. Heki [2004a] proposed a new interpretation for the NEJ fore-arc subsidence, which I will briefly introduce in the next section.

Deep Basal Erosion and Secular Subsidence of NEJ Fore Arc

Subduction (tectonic) erosion is the detachment of upper plate rock and sediment and the downward transport of this material along with the subducting lower plate. Von Huene and Scholl [1991] proposed two basic erosion mechanisms. At a trench, material collapsed from the landward slope is trapped in horst-graben structures of the subducting plate (frontal erosion). Material at the base of the upper plate may also be detached and move toward the mantle with the subducting slab (basal erosion). These two processes carry down upper plate material, make the trench retreat landward, and cause fore-arc subsidence. Heki [2004a] evaluated the amount of basal erosion using the formulation of Okada [1992] assuming compressional dislocation (fault-normal shortening) on the plate boundary. Figure 16.7 shows the model prediction curve where 15 mm/yr shortening is assumed to occur over the depth range 45–90 km (updip extent of the erosion is not well constrained, see Heki [2004a]).

According to von Huene and Lallemand [1990], the Deep Sea Drilling Project site off the Sanriku coast was subaerial at 16 Ma. This site is only 30 km distant from the trench location today. Heki [2004a] inferred the trench to have retreated 170 km in 16 myr, with an average rate of 10 mm/yr, by assuming a similar subduction zone geometry to the present (i.e., the dip angle and land-trench distance of ~200 km have been constant). If the erosion takes place uniformly over the slab dipping 30°, the average deep basal erosion rate would be 5 mm/yr. The current rate of 15 mm/yr from GPS is three times as large, i.e., erosion at this segment of NEJ might be temporarily accelerated by a subducting seamount acting as an asperity [Wells *et al.*, 2003].

Water is considered to play an essential role in basal subduction erosion [von Huene and Scholl, 1991]. A significant amount of water is released at various depths during subduction in NEJ [Iwamori, 1998]. At shallow locations, loose oceanic sediments release water as they consolidate. At greater depth (~50 km in NEJ), owing to high temperature and pressure, hydrous and clay minerals in the oceanic crust release water. This water is accommodated by the upper plate as olivine transforms to serpentine and chlorite. Serpentinized mantle is detached from the wedge mantle and is dragged down by the slab.

It eventually releases water beneath the volcanic front (~150 km in NEJ) encouraging magma genesis and arc volcanism. Geodetic data may provide a new quantitative way to explore such deep processes. A comparative study of world subduction zones, with or without subduction erosion, using vertical velocity profiles, would be meaningful in clarifying the roles of subduction erosion in convergent plate boundaries.

Transient Movements

Shortly after the start of operation of GEONET in 1994, coseismic crustal movements of two earthquakes were detected, namely the 1994 Hokkaido-Toho-Oki (Shikotan) earthquake ($M_w = 8.3$) [Tsuji *et al.*, 1995], and the 1994 Sanriku-Haruka-Oki (far-off Sanriku) earthquake ($M_w = 7.7$) [Tanioka *et al.*, 1996]. After the 1994 earthquake, GEONET detected slow crustal movement with time scales of about a year (fig. 16.9) [Heki *et al.*, 1997]. This first showed that slow fault slip is able to release seismic moment comparative to coseismic moment. Similar discoveries continued in NEJ, where seismic moment released by slow fault slip is now considered as important a process as coseismic releases. In SWJ, GEONET confirmed the existence of slow slip events not preceded by normal-speed ruptures, and some of those are found to recur fairly regularly. Here, past examples of such transient crustal movements are reviewed.

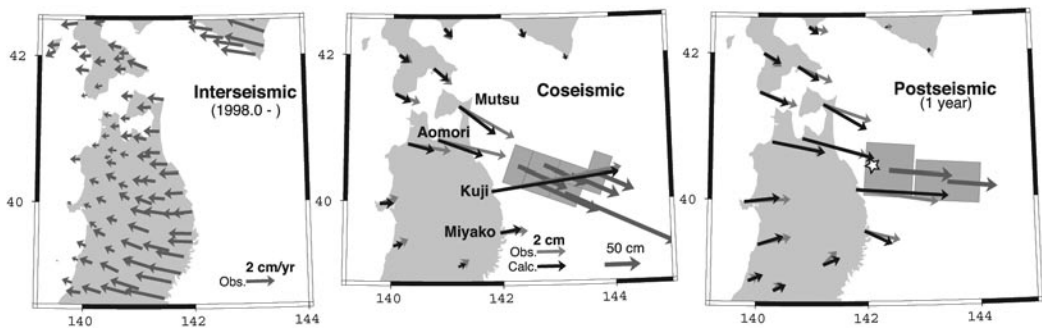


Figure 16.9 Distribution of (left) interseismic, (center) coseismic, and (right) postseismic displacement of GPS stations for the 1994 Sanriku earthquake. Since the number of GPS sites was much smaller in 1994, coseismic and postseismic movements are recorded at fewer GPS sites than interseismic movements. Postseismic movements are relative to Tsukuba over a 1-year period following the earthquake. Interseismic movements were derived using time series after 1998.0 to avoid influences of the postseismic movements (fig. 16.10). An open star in the right panel indicates the position of the small repeating earthquake [Uchida *et al.*, 2003] whose cumulative slip is shown in figure 16.10.

After Slip

Along the Japan Trench, NEJ, the distribution of past interplate earthquakes is fairly nonuniform, and cumulative slip amounts fall short of expected plate convergence rates at the trench. This suggests the existence of aseismic (“silent”) plate convergences there. Slow fault slip was first detected by quartz-tube extensometers at the Esashi Earth Tides Station, National Astronomical Observatory after the 1992 Sanriku earthquake ($M_w \sim 6.9$) [Kawasaki *et al.*, 1995]. It recorded a slow change in strain with time scale of about a day immediately after the step-like coseismic change.

After the 1994 Sanriku earthquake, GEONET detected a slow crustal movement with a time scale of about a year (fig. 16.9) [Heki *et al.*, 1997]. This was the first observation of slow fault slip in NEJ by multiple space geodetic stations, and it was found that seismic moment comparable to the coseismic moment was released during the 1-year period following the earthquake. Past earthquakes were then examined using tide gauge records, and Ueda *et al.* [2001] recognized the existence of large after slip associated with the 1978 Miyagi-Oki earthquake, similar to the 1994 Sanriku earthquake. Densification of GEONET enabled the detection of slow slip after smaller earthquakes. There was a medium-sized ($M_w \sim 6.4$) earthquake offshore east of Aomori in August 2001, for which Sato *et al.* [2004] detected a subtle (few millimeters) after-slip signal. Recent analysis by the Geographical Survey Institute [2003] also detected small after-slip signals following the 2002 November earthquake off-Miyagi (MJMA ~ 6.1). After the September 2003 Tokachi-Oki earthquake (MJMA ~ 8.0), fairly large after slip was observed to start in the region surrounding the main rupture [Takahashi *et al.*, 2004], whose total amount is still unknown.

It seems that after slip is a common phenomenon following interplate earthquakes at the Japan Trench. All interplate earthquakes during the last decade have manifested after slip. The time scale of after slip varies from 1 or 2 days for the 1992 Sanriku [Kawasaki *et al.*, 1995], to 2 months for the 2001 Aomori [Sato *et al.*, in press], to one half year for the 1994 Sanriku [Heki *et al.*, 1997]. Heki and Tamura [1997], using both strainmeter and GPS data, demonstrated a smooth transition from short- to long-term after slip of the 1994 Sanriku earthquake (fig. 16.10). These two techniques are sensitive to different time scales, and it is difficult to discuss after-slip time scales when only one kind of data are available. For example, the 1992 Sanriku event may have shown a yearlong after slip if a dense GPS array were available then (this was found to be the case by analysis of small repeating earthquakes, see the next section). The 2001 Aomori event may have shown large after slip with a time scale of a few days if a good strainmeter were available near the focal region.

Crustal deformation studies following inland earthquakes have been done by dense deployment of GPS receivers for campaign observations in and around the focal region. After slip for these earthquakes, e.g., the 1995 Kobe earthquake [Nakano and Hirahara, 1997] and the 2000 Tottori earthquake [Hashimoto *et al.*, 2003], was found to be much smaller than for interplate thrust events.

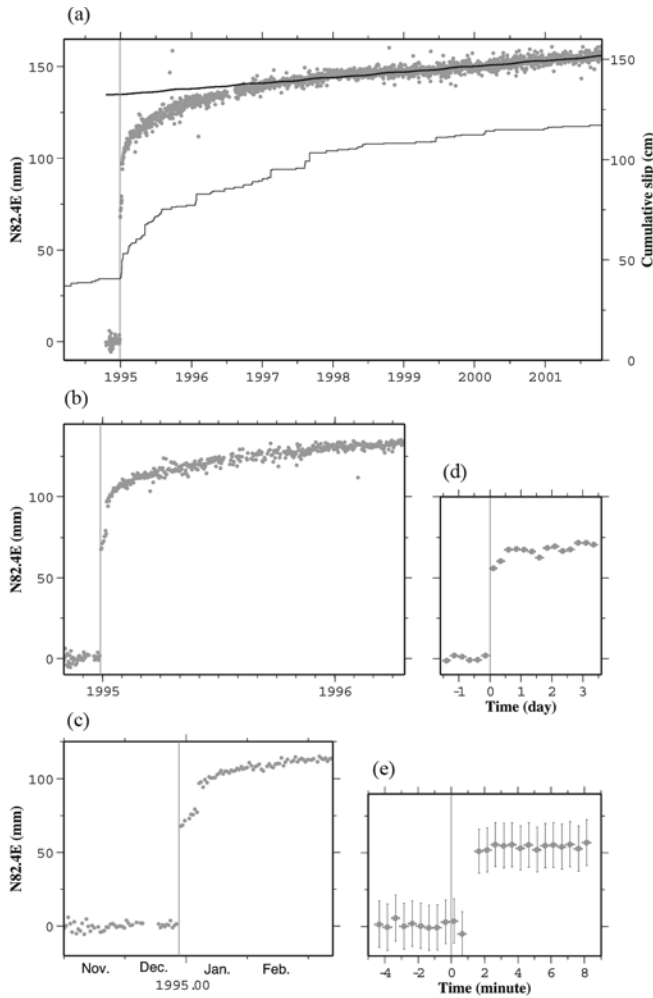


Figure 16.10 Movement of the Kuji station in the N82.4E direction viewed from the Miyako station (see fig. 16.9 for locations). They are daily solutions over (a) 6 years, (b) 1 year, (c) 4 months, and (d) quarter-daily solutions over the 5 days and epoch-wise (i.e., every 30 s) solution over (e) the ~ 12 min period. In figure 16.10a the cumulative slip of a small repeating earthquake in the afterslip area (see fig. 16.9 for position) is drawn after *Uchida et al.* [2003].

Asperities and Small Repeating Earthquakes

In addition to geodesy, seismological studies of small repeating earthquakes provide independent evidence for slow fault slip. As seen with typical repeating earthquakes, such as the M 4.8 earthquake sequence off Kamaishi [*Matsuzawa et al.*, 2002], they recur with fairly uniform intervals and similar waveforms. They are considered to be the ruptures of the same asperities that are

small in size and isolated from larger asperities [Okada *et al.*, 2003]. A transient decrease of their recurrence interval may indicate an accelerated creeping rate of that part of the plate interface. They provide useful information on after slip in several cases, e.g., GPS does not have enough sensitivity for slip occurring far off the coastline, and for earthquakes before the GPS era. For example, Igarashi *et al.* [2003] found a sudden increase in the occurrence rate of one such repeating earthquake within the 1994 Sanriku earthquake after-slip area (fig. 16.9) shortly after the earthquake (fig. 16.10). Detailed studies of such repeaters in the same region by Uchida *et al.* [2003] clarified similar accelerations after the 1992 Sanriku earthquake as well and showed propagation of the after-slip area by comparing different repeaters around the focal region.

Positions, shapes, and behaviors of larger asperities, which have caused *M* 7–8 class earthquakes in NEJ in the past, have been investigated by Yamanaka and Kikuchi [2004]. According to them, the 1994 Sanriku earthquake is caused by one of the two relatively large asperities that ruptured during the 1968 Tokachi-Oki earthquake. Figure 16.9 compares distribution of interseismic, coseismic, and postseismic crustal deformation of the 1994 Sanriku earthquake. The difference between coseismic and postseismic displacement vectors indicates that coseismic slip occurred in a rather small area corresponding to this asperity while after slip occurred over a larger area [Heki *et al.*, 1997]. Recent seismological studies of source mechanisms and after-shock distribution and a reexamination of geodetic data for this earthquake suggested that the regions of coseismic slip and after slip do not overlap; i.e., after slip occurred in the region surrounding the asperity [Yagi *et al.*, 2003]. Figure 16.10 shows the change of the ENE component of the coordinate of the Kuji GPS station relative to the Miyako station in various time scales (modified from Heki *et al.* [1997] and Heki and Tamura [1997]). The transition from coseismic to short-term postseismic movements is not seamless but distinctive, suggesting that the coseismic rupture and the after slip are processes occurring at different parts of the fault with different frictional properties. Heki and Tamura [1997] compared strain patterns and found that even the earliest part of after slip has different slip distribution from coseismic slip but similar to that of the yearlong after slip.

Silent Events and Their Recurrences

A totally silent earthquake (i.e., without normal-speed fault rupture) was first detected with GEONET in 1996, first, beneath the Boso Peninsula, central Japan [Sagiya, 1997, 2004], and second, in the Bungo Channel, SWJ, in 1997 [Hirose *et al.*, 1999]. Similar slow fault slip events found in the Cascadia subduction zone [Dragert *et al.*, 2001] seem to recur regularly with average intervals of ~14 months [Miller *et al.*, 2002] and are associated with low-frequency tremor activities [Rogers and Dragert, 2003]. Such low-frequency tremors are also discovered in Japan along the 30-km depth line of the Philippine Sea plate

slab [Obara, 2002]. However, slow crustal movements synchronized with the tremor activities have not been detected yet with GEONET.

Recently, a dike intruded along a line connecting two of the Izu Islands, Miyake, and Kozu, over a 3-month period in summer 2000, causing crustal movements of several tens of centimeters in the Kanto-Tokai region [Kaidzu *et al.*, 2000]. This was immediately followed by a slow crustal movement toward southeast in the Tokai area beginning in autumn 2000 [Ozawa *et al.*, 2002]. Its initial stage resembled to the phenomenon suggested to be the 1944 Tonankai earthquake preslip [Mogi, 1985], but the 2000 event turned out to be the onset of an episodic slow convergence event (silent earthquake) that occurred at the down-dip extension of the Tokai segment of the Nankai-Suruga Trough. The movement still goes on, and it is difficult to tell whether it is decaying or not because the signal is overprinted with seasonal components with possible interannual amplitude variations (see the last section and figure 16.14).

An important recent finding concerning silent earthquakes is their fairly regular recurrences, as revealed by GPS data in the Cascadia subduction zone [Miller *et al.*, 2002]. Exploration for such periodicity is done backward in time beyond the GPS age in Japan. Past observations of conventional ground survey suggested that silent fault slips similar to the 2000 Tokai silent event may have occurred several times, with the last one being around 1988–1990 [Kimata and Yamauchi, 1998]. This is also supported by past records of swarm earthquake activity and characteristic signals in records of a tiltmeter above the slipping region [Yamamoto *et al.*, 2005]. A silent earthquake similar to the 1996 Boso event occurred again in 2002, and old strainmeter records suggested that similar events have occurred in 1983 and 1991 [Ozawa *et al.*, 2003].

Another important finding is that deep nonvolcanic tremor activities and slow slip events occur simultaneously, as first pointed out in the Cascadia subduction zone [Rogers and Dragert, 2003]. In Japan, activities of such deep tremors were known to have certain periodicities [Obara, 2002]; e.g., it becomes active approximately every half year beneath the western Shikoku region. Using the nationwide array of borehole tiltmeters, Hirose and Obara [2005] revealed that slow changes of crustal tilts of ~ 0.1 μ rad occur together with the enhancements of tremor activities. They showed that such tilt changes indicate slow reverse slip events on what we call transition zone of the plate interface (depth 25–35 km in SWJ) where full coupling at its upper edge decays to zero at its lower edge. Surface displacements by such slow fault slips are not more than a few millimeters in amplitude, which would be difficult to detect with GEONET.

Apart from such periodicity, some of the silent earthquakes seem to have been triggered by the occurrence of nearby normal-speed earthquakes. For example, the 1997 Bungo Channel silent earthquake was preceded by two normal earthquakes in 1996 in Hyuga-nada [Yagi *et al.*, 2001; Yagi and Kikuchi, 2003]. The 2000 Tokai slow event may also have been triggered by the Miyake-Kozu dike intrusion event that should have increased the Coulomb failure stress at the Tokai event fault surface. Silent events in SWJ and Cascadia seem to

occur on the transition zone of the plate interface. In NEJ, neither such periodic silent fault slips nor deep tremor activities have been found. This might reflect observational difficulties coming from the larger depth of the transition zone in NEJ (50–65 km).

Seasonal Crustal Movements

Seasonal crustal deformation signals in the GEONET GPS site coordinate time series were studied first by *Murakami and Miyazaki* [2001]. They were highly systematic in space and suggested origins other than orbital errors that would cause signals with simpler spatial patterns. On a global scale, comprehensive studies of potential seasonal displacement signal sources were done by *Dong et al.* [2002]. Seasonal signals in northeastern Honshu were found to be due largely to snow loads along the western flanks of the backbone range by *Heki* [2001]. *Hatanaka* [2003a] pointed out the existence of seasonal signals unrelated to crustal deformation in GEONET, namely seasonal-scale changes of unknown origin and spurious displacement signals due to atmospheric gradients.

Although such periodic signals are not of tectonic origin, it is important to understand them for crustal deformation studies in active plate-boundary regions. For example, moment release history of the 2000 Tokai slow event is discussed using transient components inferred by eliminating seasonal signals [*Ozawa et al.*, 2002]. A millimeter-level after-slip signature of the 2001 off-Aomori event [*Sato et al.*, 2004] would not have been detected unless seasonal changes had been adequately removed. In these studies, elimination of seasonal components is done expecting that the same seasonal pattern repeats every year. Such interannual regularity, however, has not been well studied. In order to explore a realistic method to model seasonal components, *Heki* [2004b] evaluated various kinds of seasonally changing loads and compared the modeled variations with observed signals. Here, I briefly summarize its essential parts.

Seasonal Changes in Surface Loads

Heki [2004b] improved the approach of *Heki* [2001] by considering (1) factors other than snow, (2) the whole of Japan rather than northeastern Honshu, and (3) waveforms of seasonal load changes. *Heki* [2004b] divided the Japanese Islands into 130 blocks as large as 0.5° latitude and 0.67° longitude and estimated loads of various factors at monthly epochs for individual blocks. Then, the displacement of each GPS station was calculated as the sum of the Green's function [*Farrell*, 1972] describing the elastic response of the Earth to a point load.

Snow Load

Snow depth data are obtained daily at the Automated Meteorological Data Acquisition System (AMeDAS) sites, run by Japan Meteorological Agency.

Figure 16.11 shows the snow depth curves at three points and averages of the maximum snow depths of the last seven winters. Despite their dense deployment, these AMeDAS sites exist along inhabited valleys with altitudes lower than the regional averages. Since snow depths are highly dependent on the elevation, *Heki* [2004b] performed “altitude correction” by (1) obtaining linear relationships between snow depths and site altitudes for individual snowy prefectures and (2) performing a correction to bring the AMeDAS snow depth data to the values at the prefectural average heights. Then, the altitude-corrected snow depth data were compiled to calculate average seasonal change of snow depths within the blocks.

The average density of the snow cover increases toward the end of winter because of compaction. Using snow density data collected in situ in Japan, *Heki* [2004b] modeled the snow density to be 0.25 g/cm^3 on 1 December and to increase linearly with time reaching 0.4 g/cm^3 on 31 March. This time-dependent model density was used to convert snow depths to loads (fig. 16.12). Large snow loads are distributed along the northwestern flanks of the back-

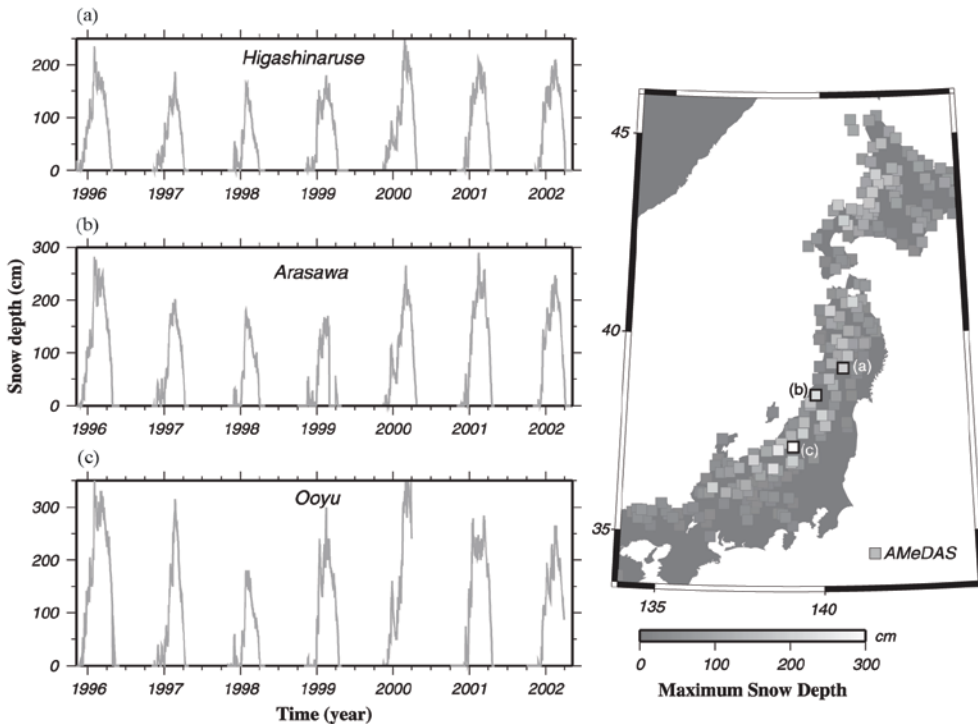


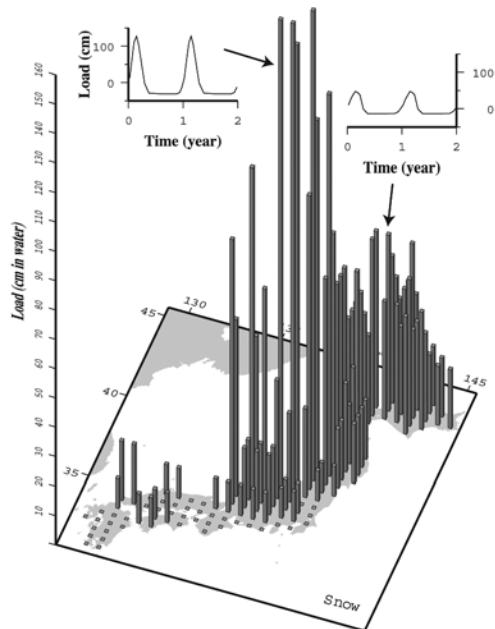
Figure 16.11 Daily snow depth measurements at three AMeDAS sites, (a) Higashinaruse (Akita Prefecture), (b) Arasawa (Yamagata Prefecture), and (c) Ooyu (Niigata Prefecture), indicated as squares with bold frames in the map, from north to south, over the (left) seven winter seasons 1996–2002 (left graphs), and (right) distribution of the average of the maximum snow depths of the seven winters at the AMeDAS sites equipped with snow depth meters.

bone range, while they are almost absent along the Pacific coast and in SWJ. As shown in the insets of figure 16.12, snow load changes are characterized by strong peak in winter and relatively flat period during the rest of the seasons.

Other Loads The second largest seasonal changing load is the atmosphere. Unlike snow, atmospheric loading exists both on the land and ocean, but at relatively long periods (e.g., annual frequency), pressure changes are exerted only on the land area (inverted barometer). *Heki* [2004b] calculated monthly mean pressures for individual blocks, using meteorological data at 80 sites from *National Astronomical Observatory* [2002]. In general, pressure tends to be higher in winter in Japan, and the amplitude of seasonal variation increases toward the west. The peak-to-peak changes amount to 1.5 kPa (~15-cm water column) in Kyushu but are <1 kPa in NEJ. They are smaller than snow loads but are responsible for the main seasonal load in snow-free parts of Japan.

Heki [2004b] also modeled seasonal variation of soil moisture throughout Japan, using a simple model based on the potential evapotranspiration (PET) [Thornthwaite, 1948], precipitation, and the water-holding capacity of soil [Milly, 1994]. Simulation of seasonal change in soil water performed with monthly time steps at various points in Japan showed that the load changes are smaller than atmosphere in most regions. Their peak-to-peak changes are largest in the inland area of southwestern Japan and Hokkaido but do not exceed 1 kPa. *Heki* [2004b] also compiled capacities and coordinates of 546 dams that can accommodate more than five million tons of water and calculated sea-

Figure 16.12 Distribution of the maximum snow load in Japan divided into 130 blocks as large as 0.5° in latitude and 0.67° in longitude, obtained as the average of the last seven winters. Insets are the seasonal snow load changes at the two selected blocks indicated by arrows. Since the annual averages are adjusted to zero there, loads take negative values during summer.



sonal variations of the load assuming the typical water-level change patterns of Japanese dams. The peak-to-peak amplitudes of the dam load are the largest in the mountain area of central Japan. However, they are ~ 1 kPa at most and are much less than the two major contributors, i.e., snow and atmosphere.

Sea surface height (SSH) in September is known to be higher than in March by 20 cm or more along the Pacific coast of Japan [Okada, 1982; Kato, 1983]. This includes thermal expansion irrelevant to load changes, and Sato *et al.* [2001] removed it assuming uniform thermal steric coefficient of 6.0 mm/deg. After applying such a correction, SSH is found to be almost stationary throughout a year in the Japan Sea. However, a large summer increase in SSH still remains in the Pacific Ocean. This seasonal ocean load change gives rise to a seasonal translation of the whole Japanese Islands by ~ 1 mm, but crustal deformation within the Japanese Islands does not much exceed those by soil moisture and dam. Apart from loads, Munekane *et al.* [2003] revealed that inflation and deflation of soil by seasonal extraction of groundwater for agricultural purposes cause vertical movements of GPS sites with amplitudes exceeding 10 mm at certain regions including Tsukuba. This can be confirmed by collocating water level meters of deep wells with GPS receivers [Ohtani *et al.*, 2000], and the areal extent of such regions should be clarified in future by using inSAR technique.

Apparent Seasonal Crustal Movement In addition to real seasonal crustal deformation due to surface load, Hatanaka [2003a] found that the entire GPS network manifests annual cycles of uniform expansion in summer and contraction in winter (seasonal scale change) of ~ 5 – 6 part per billion (ppb). Isotropic contraction causes substantial shortening of arc-parallel baselines, which lets us discriminate scale changes easily from load changes characterized by arc-normal contractions [Heki, 2004b]. Seasonal degree-one deformation [Blewitt *et al.*, 2001] causes an apparent scale change in Japan but its amplitude is < 1 ppb. Hatanaka [2003a] considered the scale change as an artifact irrelevant to deformation of the real Earth, e.g., scale change caused by an error in absolute atmospheric delay [Beutler *et al.*, 1988]. Heki [2004b] showed that the seasonal-scale change patterns are similar from year to year and made an empirical model to enable a seasonal-scale correction.

In addition to seasonal-scale changes, Hatanaka [2003a] pointed out that atmospheric delay gradients [Miyazaki *et al.*, 2003] are significant in the north-south direction at stations along the Pacific coast of SWJ. GSI does not estimate atmospheric gradients in their official GEONET solutions [Hatanaka, 2003b]. Atmospheric delay gradients tend to cause apparent northward movement of the Pacific side stations in winter relative to the Japan Sea side. This contributes to the arc-normal winter contraction in SWJ and enhances the signals of seasonally changing loads. By comparing solutions with and without estimation of atmospheric gradient parameters, Hatanaka [2003a] found that this effect may contribute to seasonal signals by up to a few millimeters.

Comparison With GPS Observations

Heki [2004b] calculated the effect of the sum of crustal deformation due to seasonal changing loads including snow, atmosphere, soil moisture, dam, and SSH and contributions from the seasonal-scale changes on baseline lengths. Figure 16.13 compares modeled seasonal signals with those observed by GEONET (lengths of five arc-normal baselines) from the newest solution based on the improved analysis strategy [Hatanaka, 2003b]. Snow-induced signals are characterized by sharp negative peaks in winter and a relatively flat period from spring to autumn. Other components, mainly scale and atmospheric load, bring about a broad positive peak in summer making the total waveform a mild one. In total, arc-normal contraction of up to 4–5 mm across the backbone range is expected in winter in NEJ. This feature seems to be well reproduced in the real data. The southernmost baseline (baseline E, fig. 16.13) show somewhat larger seasonal variations than predicted. Part of this discrepancy may come from the north-south atmospheric gradient at southern stations. Arc-parallel baselines are more affected by scale changes, although snow load has significant contributions in NEJ. Unlike baseline length changes that mainly reflect horizontal coordinates, vertical components are less affected

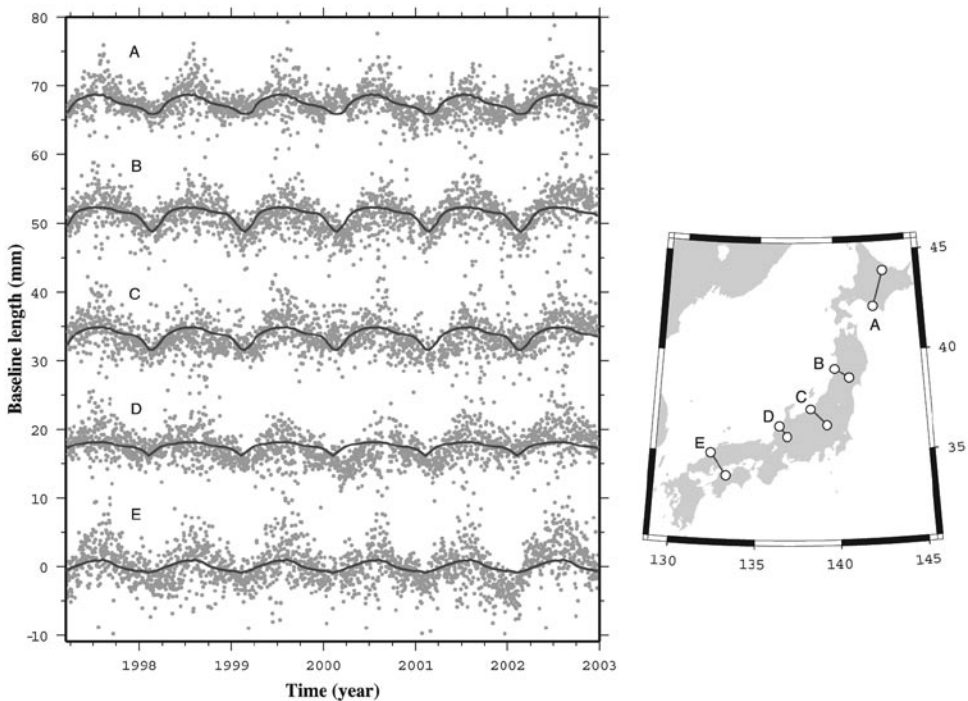


Figure 16.13 Seasonal change in lengths for five arc-normal baselines shown in the right map. Dots are daily solution of GPS (secular trends are removed beforehand), while curves denote model seasonal variation curves calculated by combining contributions from scale, snow, atmosphere, soil moisture, dam, and ocean.

by scale changes and respond mainly to change in load. *Heki* [2004b] showed that seasonal vertical movements along the snowiest zone show subsidence in winter of ~ 10 mm. Some sites, such as Tsukuba, show vertical seasonal movements larger than model expectations, which may reflect seasonal change in groundwater levels.

Relationship with Earthquake Occurrence Seasonality

Seismic activity in some regions in Japan is known to change seasonally [*Mogi*, 1969; *Okada*, 1982]. Using the newest historical earthquake catalog, *Heki* [2003] confirmed the tendency that inland earthquakes $M > 7.0$ in snow-covered regions in Japan occur more in spring and summer, as originally suggested by *Okada* [1982], and hypothesized that they may have been triggered by removal of snow load by spring thaw. As explained in the previous section, snow is by far the largest seasonally changing load in Japan. This justifies the approach by *Heki* [2003], in which only snow effects are considered. To verify their causal relationship, however, we need to solve several problems, e.g., ambiguous seasonality for smaller ($M < 7.0$) earthquakes, insufficient statistical significance due to a small number of historical large inland earthquakes, and so on.

Interplate thrust events along the Nankai, Suruga, and Sagami Troughs are known to occur more in autumn and winter [*Ohtake and Nakahara*, 1999]. This is qualitatively consistent with the seasonal change of nontidal oceanic loads; the SSH shows maximum in August/September [*Okada*, 1982], and the highest seismicity in December coincide with the period of the highest rate of load decrease ($\frac{1}{4}$ cycle after the load peak). However, such seasonal concentration is not so clear for interplate earthquakes at the Japan Trench, NEJ; they seem to have a small peak in March in addition to the broad peak in autumn/winter similar to SWJ. Deployment of ocean bottom pressure gauges on the landward slope of the Japan Trench is in progress so that we can monitor in situ water mass changes above the sensor [e.g., *Fujimoto et al.*, 2003]. Such data will help us conclude if there is causal relationship between change in ocean loads and interplate earthquake occurrences in the future.

Conclusions

About 10 years of the GEONET GPS data have clarified various new aspects of crustal dynamics and earthquake physics in subduction zones. The large-scale plate tectonic setting of the Japanese Islands is still controversial, but there is a general agreement that Japan is divided into two plates colliding with each other somewhere in central Japan. This has a certain influence on the discussion on the seismic moment budget along the Nankai-Suruga Trough. Interseismic crustal movements are generally consistent with those predicted by slip deficits at the seismogenic parts of the plate boundaries. Figure 16.14

shows the movement in a certain horizontal direction of Hamamatsu relative to Oogata in which all of secular, transient, and periodic crustal deformation signals discussed in this paper are present. There the secular component corresponds to the movement of the Hamamatsu station owing to interseismic elastic straining by the subducting PH slab.

Vertical velocities in the fore arc of NEJ are found to deviate negatively from the model, suggesting the existence of a certain geological process responsible for its secular subsidence. This might indicate the thinning of the upper plate at depths 45–90 km due to basal subduction erosion, which may be a manifestation of the process at depth that mantle material serpentinized by water released from the slab is detached from the upper plate and transported downward.

One of the most important findings by GPS is the discovery of aseismic slow faulting. In NEJ, they often occur immediately after normal-speed earthquakes over areas surrounding asperities (after slips). Their time constants seem to range from days to a year. Recent studies of small repeating earthquakes have given independent support to this view. In central and southwestern Japan, slow slip tends to occur as single events (silent earthquakes). Many of those have been found to occur repeatedly with recurrence inter-

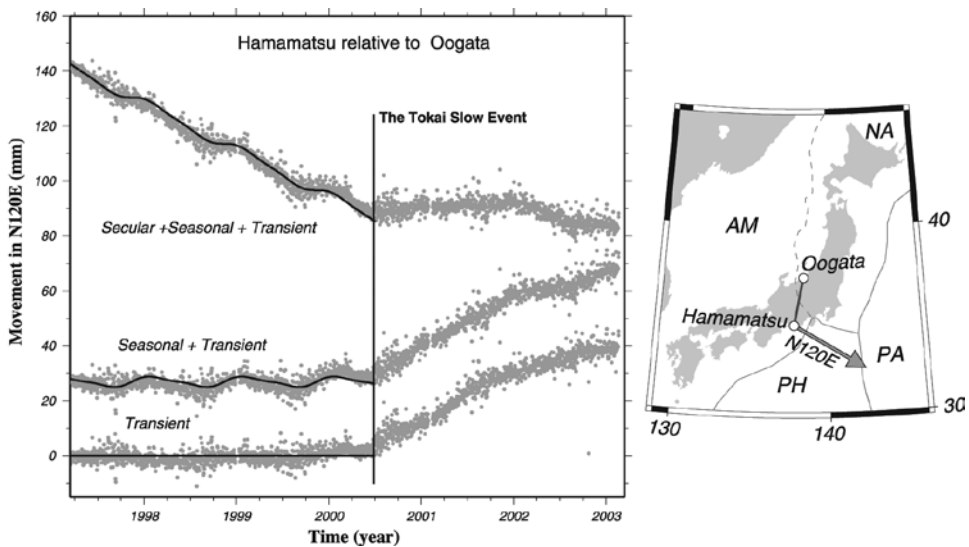


Figure 16.14 Movement of the horizontal coordinate of the Hamamatsu GPS station, in the Tokai area, with respect to the Oogata station (see the right map for location). (top) The raw data includes secular, transient, and seasonal components. In the middle curve, the secular trend is removed. In the lower curve, seasonal changes are also removed. Seasonal and secular movements are inferred using the time series before the onset of the Tokai slow event in the 2000 autumn [Ozawa *et al.*, 2002]. Solid lines indicate modeled secular and seasonal changes.

vals ranging from half year (western Shikoku), 13 months (Cascadia), 6 years (Boso Peninsula), to >10 years (Tokai). In western Shikoku and Cascadia they are accompanied by deep nonvolcanic tremor activities, which suggests a causal relationship between water released from the subducting slab and the occurrences of slow slip. In figure 16.14 the sudden departure from the normal trend in the middle of 2000 shows the onset of the 2000 Tokai slow event recorded at the Hamamatsu station.

Mechanisms of seasonal crustal deformation due to changes of surface loads are being understood, but mechanisms responsible for seasonal-scale changes of a few ppb in Japan are yet to be investigated. The top curve of figure 16.14 includes seasonal components whose large portion comes from snow load changes near Oogata. The seasonal signals are removed in the bottom curve of figure 16.14 by modeling them with annual and semiannual components using time series before the onset of the 2000 Tokai event. It is important to understand seasonal signals and their interannual variations in order to study subtle transient signals, e.g., slow fault slips at depth. For the seasonal changes of seismic activities, a century-long issue of Japanese seismology, quantitative studies of influence of seasonal load changes on seismicity are in progress.

Acknowledgments

I thank Tim Dixon (University of Miami) and Seth Stein (Northwestern University) for inviting me to present a review at the Snowbird meeting on which this paper is based. Naoki Uchida (Tohoku University) sent me data on the repeating earthquakes. I also thank Jeff Freymueller (University of Alaska) and an anonymous referee for critical reviews of the manuscript.

References

- Altamimi, Z., P. Sillard, and C. Boucher (2002), ITRF2000: A new release of the International Terrestrial Reference Frame for earth science applications, *J. Geophys. Res.*, 107(B10), 2214, doi:10.1029/2001JB000561.
- Aoki, Y., and C. H. Scholz (2003), Vertical deformation of the Japanese islands, 1996–1999, *J. Geophys. Res.*, 108(B5), 2257, doi:10.1029/2002JB002129.
- Beutler, G., I. Bauersima, W. Gurtner, M. Rothacher, T. Schildknecht, and A. Geiger (1988), Atmospheric refraction and other important biases in GPS carrier phase observations, in *Atmospheric Effects on Geodetic Space Measurements, Monogr. Ser.*, vol. 12, edited by F. K. Brunner, p. 26, Sch. of Surv., Univ. New South Wales, Kensington.
- Blewitt, G., D. Lavallée, P. Clarke, and K. Nurutdinov (2001), A new global mode of earth deformation: Seasonal cycle detected. *Science*, 294, 2342–2345.
- Cohen, S. C. (1994), Evaluation of the importance of model features for cyclic eformation due to dip-slip faulting, *Geophys. J. Int.*, 119, 831–841.
- DeMets, C., D. Argus, S. Stein, and R. Gordon (1990), Current plate motions, *Geophys. J. Int.*, 101, 425–478.

- Dong, D., P. Fang, Y. Bock, M. K. Cheng, and S. Miyazaki (2002), Anatomy of apparent seasonal variations from GPS-derived site position time series, *J. Geophys. Res.*, 107(B4), 2075, doi:10.1029/2001JB000573.
- Dragert, H., K. Wang, and T.S. James (2001), A silent slip event on the deeper Cascadia subduction interface, *Science*, 292, 1525–1528.
- Earthquake Research Committee (1998), Seismic activity in Japan—Regional perspectives on the characteristics of destructive earthquakes (excerpt), report, 222 pp., Headquarters of the Earthquake Res. Promotion, Prime Minist. Off., Gov. of Jpn., Tokyo.
- Farrell, W. E. (1972), Deformation of the Earth by surface loads. *Rev. Geophys.*, 10, 761–797.
- Fujimoto, H., M. Mochizuki, K. Mitsuzawa, T. Tamaki, and T. Sato (2003), Ocean bottom pressure variations in the southeastern Pacific following the 1997–98 El Niño event, *Geophys. Res. Lett.*, 30, 1456, doi:10.1029/2002GL016677.
- Geographical Survey Institute (2002), Crustal deformation of entire Japan, in *Report of the Coordinating Committee for Earthquake Prediction*, vol. 68, pp.504–533, Tsukuba, Japan.
- Geographical Survey Institute (2003), Crustal movements in the Tohoku District, in *Report of the Coordinating Committee for Earthquake Prediction*, vol. 70, pp. 45–68, Tsukuba, Japan.
- Hasegawa, A., D. Zhao, S. Hori, A. Yamamoto, and S. Horiuchi (1991), Deep structure of the northeastern Japan arc and its relationship to seismic and volcanic activity, *Nature*, 352, 683–689.
- Hashimoto, M., T. Ito, T. Tabei, and T. Sagiya (2003), Postseismic deformation following the 2000 Western Tottori earthquake, southwest Japan, using GEONET and urgent campaign GPS data, paper presented at the 23rd IUGG General Assembly, Sapporo, Japan, 7 July.
- Hatanaka, Y. (2003a), Seasonal variation of scale of GEONET network and ZTD biases, paper presented at the 23rd IUGG General Assembly, Sapporo, Japan, 7 July.
- Hatanaka, Y. (2003b), Improvement of the analysis strategy of GEONET, *Bull. Geogr. Surv. Inst.*, 49, 11–37.
- Heki, K. (2001), Seasonal modulation of interseismic stress buildup in northeastern Japan driven by snow loads, *Science*, 293, 89–92.
- Heki, K. (2003), Snow load and seasonal variation of earthquake occurrence in Japan, *Earth Planet. Sci. Lett.*, 207, 159–164.
- Heki, K. (2004a), Space geodetic observation of deep basal subduction erosion in northeastern Japan, *Earth Planet. Sci. Lett.*, 219, 13–20.
- Heki, K. (2004b), Dense GPS array as a new sensor of seasonal changes of surface loads, in *The State of the Planet: Frontiers and Challenges in Geophysics*, *Geophys. Monogr. Ser.*, vol. 150, edited by R. S. J. Sparks and C. J. Hawkesworth, pp. 177–196, AGU, Washington, D. C.
- Heki, K., and S. Miyazaki (2001), Plate convergence and long-term crustal deformation in central Japan, *Geophys. Res. Lett.*, 28, 2313–2316.
- Heki, K., and Y. Tamura (1997), Short term afterslip in the 1994 Sanriku-Haruka-Oki earthquake, *Geophys. Res. Lett.*, 24, 3285–3288.
- Heki, K., H. Tsuji, and S. Miyazaki (1997), Silent fault slip following an interplate thrust earthquake at the Japan Trench, *Nature*, 386, 595–597.
- Heki, K., S. Miyazaki, H. Takahashi, M. Kasahara, F. Kimata, S. Miura, N. Vasilenko, A. Ivashchenko, and K. An (1999), The Amurian Plate motion and current plate kinematics in eastern Asia, *J. Geophys. Res.*, 104, 29,147–29,155.
- Hirose, H. and K. Obara (2005), Repeating short- and long-term slow slip events with deep tremor activity around the Bungo channel region, southwest Japan, *Earth Planets Space*, 57, 961–972.
- Hirose, H., K. Hirahara, F. Kimata, N. Fujii, and S. Miyazaki (1999), A slow thrust slip event following the two 1996 Hyuganada earthquakes beneath the Bungo Channel, southwest Japan, *Geophys. Res. Lett.*, 26, 3237–3240.

- Igarashi, T., T. Matsuzawa, and A. Hasegawa (2003), Repeating earthquakes and interplate aseismic slip in the northeastern Japan subduction zone, *J. Geophys. Res.*, 108(B5), 2249, doi:10.1029/2002JB001920.
- Ishibashi, K. (1981), Specification of a soon-to-occur seismic faulting in the Tokai district, central Japan, based upon seismotectonics, in *Earthquake Prediction: An International Review, Maurice Ewing Ser.*, vol. 4, D. W. Simpson and P. G. Richards, pp. 297–332, AGU, Washington, D. C.
- Iwamori, H. (1998), Transportation of H₂O and melting in subduction zones, *Earth Planet. Sci. Lett.*, 160, 65–80.
- Kaidzu, M., T. Nishimura, M. Murakami, S. Ozawa, T. Sagiya, H. Yarai, and T. Imakiire (2000), Crustal deformation associated with crustal activities in the Northern Izu Islands area during the summer, 2000, *Earth Planets Space*, 52, ix–xviii.
- Kato, T. (1983), Secular and earthquake-related vertical crustal movements in Japan as deduced from tidal records [1951–1981]. *Tectonophysics*, 97, 183–200.
- Kawasaki, I., Y. Asai, Y. Tamura, T. Sagiya, N. Mikami, Y. Okada, M. Sakata, and M. Kasahara (1995), The 1992 Sanriku-Oki, Japan, ultra-slow earthquake, *J. Phys. Earth*, 43, 105–116.
- Kimata, F., and T. Yamauchi (1998), Time series of line lengths on the baselines in the Tokai region detected by EDM in the period of 1978 to 1997 (in Japanese with English abstract), *J. Seismol. Soc. Jpn.*, 51(35), 229–232.
- Kobayashi, Y. (1983), On the initiation of subduction of plates (in Japanese), *Earth Monthly*, 5, 510–514.
- Kogan, M., G. M. Steblov, R. W. King, T. A. Herring, D. I. Frolov, S. G. Egorov, V. Ye. Levin, A. Lerner-Lam, and A. Jones (2000), Geodetic constraints on the rigidity and relative motion of Eurasia and North America, *Geophys. Res. Lett.*, 27, 2041–2044.
- Larson, K. M., P. Bodin, and J. Gombert (2003) Using 1-Hz GPS data to measure deformations caused by the Denali Fault earthquake, *Science*, 300, 1421–1424.
- Matsuzawa, T., T. Igarashi, and A. Hasegawa (2002), Characteristic small-earthquake sequence off Sanriku, northeastern Honshu, Japan, *Geophys. Res. Lett.*, 29(11), 1543, doi:10.1029/2001GL014632.
- Mazzotti, S., X. LePichon, P. Henry, and S. Miyazaki (2000), Full interseismic locking of the Nankai and Japan-West Kurile subduction zones: An analysis of uniform elastic strain accumulation in Japan constrained by permanent GPS, *J. Geophys. Res.*, 105, 13,159–13,177.
- Miller, M. M., T. Melbourne, D. J. Johnson, and W. Q. Sumner (2002), Periodic slow earthquakes from the Cascadia subduction zone, *Science*, 295, 2423–2423.
- Milly, P. C. D. (1994), Climate, soil water storage, and the average annual water balance. *Water Resour. Res.*, 30, 2143–2156.
- Mitrovica, J. X., M. E. Tamisiea, J. L. Davis, and G. A. Milne (2001), Recent mass balance of polar ice sheets inferred from patterns of global sea-level change, *Nature*, 409, 1026–1029.
- Miyazaki, S., and K. Heki (2001), Crustal velocity field of southwest Japan: Subduction and arc-arc collision, *J. Geophys. Res.*, 106, 4305–4326.
- Miyazaki, S., T. Iwabuchi, K. Heki, and I. Naito (2003), An impact of estimating tropospheric gradient on precise positioning in summer using the Japanese nationwide GPS array, *J. Geophys. Res.*, 108(B7), 2335, doi:10.1029/2000JB000113.
- Mogi, K. (1969), Monthly distribution of large earthquakes in Japan (in Japanese with English abstract), *Bull. Earthquake Res. Inst. Univ. Tokyo*, 47, 419–427.
- Mogi, K. (1985), Temporal variation of crustal deformation during the days preceding a thrust-type great earthquake – the 1944 Tonankai earthquake of magnitude 8.1. *Pure Appl. Geophys.*, 122, 765–780.
- Munekane, H., M. Tobita, K. Takashima, S. Matsuzaka, Y. Kuroishi, and Y. Masaki (2003), Groundwater-driven vertical movement in Tsukuba detected by GPS, paper presented at the Fall Meeting, AGU, San Francisco, Calif., 12 Dec.

- Murakami, M., and S. Miyazaki (2001), Periodicity of strain accumulation detected by permanent GPS array: Possible relationship to seasonality of major earthquakes' occurrence, *Geophys. Res. Lett.*, *28*, 2983–2986.
- Nakamura, K. (1983), Possible nascent trench along the eastern Japan Sea as the convergent boundary between Eurasian and North American plates (in Japanese with English abstract), *Bull. Earthq. Res. Inst. Univ. Tokyo*, *58*, 711–722.
- Nakano, T., and K. Hirahara (1997), GPS observation of postseismic deformation for the 1995 Hyogo-ken Nanbu earthquake, Japan, *Geophys. Res. Lett.*, *24*, 503–506.
- National Astronomical Observatory (2002), *Chronological Scientific Tables*, vol. 76, 942 pp., Maruzen, Tokyo.
- Nishimura, T., et al. (2000), Distribution of seismic coupling on the subducting plate boundary in northeastern Japan inferred from GPS observations, *Tectonophysics*, *323*, 217–238.
- Obara, K. (2002), Nonvolcanic deep tremor associated with subduction in southwest Japan, *Science*, *296*, 1579–1681.
- Ohtake, M., and H. Nakahara (1999), Seasonality of great earthquake occurrence at the northwestern margin of the Philippine Sea plate, *Pure Appl. Geophys.*, *155*, 689–700.
- Ohtani, R., N. Koizumi, N. Matsumoto, and E. Tsukuda (2000), Preliminary results from permanent GPS array by the Geological Survey of Japan in conjunction with groundwater-level observations, *Earth Planets Space*, *52*, 663–668.
- Okada, M. (1982), Seasonal variation in the occurrence rate of large earthquakes in and near Japan and its regional differences (in Japanese with English abstract), *J. Seismol. Soc. Jpn.*, *35*, 53–64.
- Okada, Y. (1992), Internal deformation due to shear and tensile faults in a half-space, *Bull. Seismol. Soc. Am.*, *82*, 1018–1040.
- Okada, T., T. Matsuzawa, and A. Hasegawa (2003), Comparison of source areas of $M4.8 \pm 0.1$ repeating earthquakes off Kamaishi, NE Japan: Are asperities persistent features? *Earth Planet. Sci. Lett.*, *213*, 361–374.
- Ozawa, S., M. Murakami, M. Kaidzu, T. Tada, T. Sagiya, Y. Hatanaka, H. Yarai, and T. Nishimura (2002), Detection and monitoring of ongoing aseismic slip in the Tokai Region, Central Japan, *Science*, *298*, 1009–1012.
- Ozawa, S., S. Miyazaki, Y. Hatanaka, T. Imakiire, M. Kaidzu, and M. Murakami (2003), Characteristic silent earthquakes in the eastern part of the Boso Peninsula, central Japan, *Geophys. Res. Lett.*, *30*(6), 1230, doi:10.1029/2002GL016665.
- Rogers, G., and H. Dragert (2003), Episodic tremor and slip on the Cascadia subduction zone: the chatter of silent slip, *Science*, *300*, 1942–1943.
- Sagiya, T. (1997), Boso peninsula silent earthquake of May 1996, *Eos Trans. AGU*, *78*(46), Fall Meet. Suppl., Abstract G42A-07.
- Sagiya, T. (1999), Interplate coupling in the Tokai District, central Japan, deduced from continuous GPS data, *Geophys. Res. Lett.*, *26*, 2315–2318.
- Sagiya, T. (2004) Interplate coupling in the Kanto District, central Japan, and the Boso Peninsula silent earthquake in May 1996, *Pure Appl. Geophys.*, *161*, 2327–2342.
- Sagiya, T., S. Miyazaki, and T. Tada (2000), Continuous GPS array and present-day crustal deformation of Japan, *Pure Appl. Geophys.*, *157*, 2303–2322.
- Sangawa, A. (1993), The paleo-earthquake study using traces of the liquefaction (in Japanese), *Quat. Res.*, *32*, 249–255.
- Sato, T., Y. Fukuda, Y. Aoyama, H. McQueen, K. Shibuya, Y. Tamura, K. Asari, and M. Ooe (2001), On the observed annual gravity variation and the effect of sea surface height variations, *Phys. Earth Planet. Inter.*, *123*, 45–63.
- Sato, T., K. Imanishi, N. Kato, and T. Sagiya (2004), Detection of a slow slip event from small signal in GPS data, *Geophys. Res. Lett.*, *31*, L05606, doi:10.1029/2004GL019514.
- Savage, J. C. (1983), A dislocation model of strain accumulation and release at a subduction zone, *J. Geophys. Res.*, *88*, 4984–4996.

- Seno, T., T. Sakurai, and S. Stein (1996), Can the Okhotsk plate be discriminated from the North American plate? *J. Geophys. Res.*, *101*, 11,305–11,315.
- Suwa, Y., S. Miura, A. Hasegawa, T. Sato, and K. Tachibana (2003), Inter-plate coupling beneath the NE Japan arc inferred from 3 dimensional crustal deformation, paper presented at the 23rd IUGG General Assembly, AGU, Sapporo, Japan, 8 July.
- Takahashi, H., et al. (2004), GPS observation of the first month of postseismic crustal deformation associated with the 2003 Tokachi-Oki earthquake [MJMA8.0], off southeastern Hokkaido, Japan, *Earth Planets Space*, *56*, 377–382.
- Tanioka, Y., L. Ruff, and K. Satake (1996), The Sanriku-oki, Japan, earthquake of December 28, 1994 [*Mw* 7.7]: Rupture of a different asperity from a previous earthquake, *Geophys. Res. Lett.* *23*:1465-1468.
- Thornthwaite, C. W. (1948), An approach toward a rational classification of climate, *Geogr. Rev.*, *38*, 55–94.
- Tsuji, H., Y. Hatanaka, T. Sagiya, and M. Hashimoto (1995), Coseismic crustal deformation from the 1994 Hokkaido-Toho-Oki earthquake monitored by a nationwide continuous GPS array in Japan, *Geophys. Res. Lett.*, *22*, 1669–1672.
- Uchida, N., T. Matsuzawa, A. Hasegawa, and T. Igarashi (2003), Interplate quasi-static slip off Sanriku, NE Japan, estimated from repeating earthquakes, *Geophys. Res. Lett.*, *30*(15), 1801, doi:10.1029/2003GL017452.
- Ueda, H., M. Ohtake, and H. Sato (2001), Afterslip of the plate interface following the 1978 Miyagi-Oki, Japan, earthquake, as revealed from geodetic measurement data, *Tectonophysics*, *338*, 45–57.
- von Huene, R., and D. Scholl (1991), Observations at convergent margins concerning sediment subduction, subduction erosion, and the growth of continental crust, *Rev. Geophys.*, *29*, 279–316.
- von Huene, R., and S. Lallemand (1990), Tectonic erosion along the Japan and Peru convergent margins, *Geol. Soc. Am. Bull.*, *102*, 704–720.
- Wells, R. E., R. J. Blakely, Y. Sugiyama, D. W. Scholl, and P. A. Dinterman (2003), Basin-centered asperities in great subduction zone earthquakes: A link between slip, subsidence, and subduction erosion? *J. Geophys. Res.*, *108*(B5), 2507, doi:10.1029/2002JB002072.
- Yagi, Y., and M. Kikuchi (2003), Partitioning between seismogenic and aseismic slip as highlighted from slow slip events in Hyuga-nada, Japan, *Geophys. Res. Lett.*, *30*(2), 1087, doi:10.1029/2002GL015664.
- Yagi, Y., M. Kikuchi, and T. Sagiya (2001), Co-seismic slip, post-seismic slip, and aftershocks associated with two large earthquakes in 1996 Hyuga-nada, Japan, *Earth Planets Space*, *53*, 793–803.
- Yagi, Y., M. Kikuchi, and T. Nishimura (2003), Co-seismic slip, post-seismic slip, and largest aftershock associated with the 1994 Sanriku-haruka-oki, Japan, earthquake, *Geophys. Res. Lett.*, *30*(22), 2177, doi:10.1029/2003GL018189.
- Yamamoto, E., S. Matsumura, and T. Ohkubo (2005), A slow slip event in the Tokai area detected by tilt and seismic observation and its possible recurrence, *Earth Planets Space*, *57*, 917–923.
- Yamanaka, K., and M. Kikuchi (2004), Asperity map along the subduction zone in northeastern Japan inferred from regional seismic data, *J. Geophys. Res.*, *109*, B07307, doi:10.1029/2003JB002683.